JOURNAL OF GEOPHYSICAL RESEARCH, VOL. 102, NO. A1, PAGES 307-318, JANUARY 1, 1997

Structures in ionospheric number density and velocity associated with polar cap ionization patches

Ö. Kivanç and R. A. Heelis

William B. Hanson Center for Space Sciences, University of Texas at Dallas, Richardson

Abstract. Spectral characteristics of polar cap F region irregularities on large density gradients associated with polar ionization patches are studied using in situ measurements made by the Dynamics Explorer 2 (DE 2) spacecraft. The 18 patches studied in this paper were identified by the algorithm introduced by *Coley and Heelis* [1995], and they were encountered during midnight-noon passes of the spacecraft. Density and velocity spectra associated with these antisunward convecting patches are analyzed in detail. Observations indicate the presence of structure on most patches regardless of the distance between the patch and the cusp where they are believed to develop. Existence of structure on both leading and trailing edges is established when such edges exist. Results, which show no large dependence of $\Delta N/N$ power on the sign of the edge gradient ∇N, do not allow the identification of leading and trailing edges of the patch. The $\Delta N/N$ is an increasing function of ∇N regardless of the sign of the gradient. The correlation between $\Delta N/N$ and ΔV is generally poor, but for a given intensity in ΔV, $\Delta N/N$ maximizes in regions of large gradients in N. There is evidence for the presence of unstructured patches that seem to coexist with unstructured horizontal velocities. Slightly smaller spectral indices for trailing edges support the presence of the E×B drift instability. Although this instability is found to be operating in some cases, results suggest that stirring may be a significant contributor to kilometer-size structures in the polar cap.

1. Introduction

Production, loss, and transport processes are responsible for the largest scale size plasma structures observed in the high-latitude ionosphere [*Kelley*, 1989]. With wavelengths ranging from 30 to 1000 km, these large-scale features have recently been identified as the seat for smaller-scale kilometer-size structures [*Tsunoda*, 1988]. In the presence of large gradients due to larger-scale structures, convective plasma processes such as fluid interchange instabilities [*Keskinen and Ossakow*, 1983] and turbulent mixing [*Kintner and Seyler*, 1985] are dominant mechanisms that produce a spectrum of irregularities that range in scales from 10 km down to the ion gyroradius. Polar cap ionization patches are among such large-scale structures that produce the suitable background conditions for these mechanisms to operate.

Existence of polar cap F layer ionization patches with horizontal scale sizes ranging from a few hundred kilometers to 1000 km have been reported over the last 30 years in literature since *Hill* [1966]. Later observations [e.g., *Weber et al.*, 1984] indicate that these plasma enhancements are not locally produced by structured particle precipitation, but instead they are produced near or equatorward of the dayside auroral zone, and they drift antisunward into the winter polar cap with E×B velocities. Lower-latitude studies [e.g., *Foster and Doupnik*, 1984] observed the poleward convection of solar-produced plasma through the cusp and suggested this as a source of enhanced F layer plasma in the polar ionosphere. Several different generation mechanisms are suggested for the polar cap ionization patches. Penetration of dayside plasma into the nightside under a large eastward electric field, together with a large variation in the B_z or B_y component of the interplanetary magnetic field (IMF), is presented as one mechanism by *Tsunoda* [1988]. Simulations of similar time varying convection patterns [*Anderson et al.*, 1988; *Sojka et al.*, 1993; *Decker et al.*, 1994] have shown that such variations can detach the plasma from the dayside through changes in the polar cap radius that result from changes in the cross-tail potential. Another mechanism that leads to the formation of patches in geomagnetically conjugate regions is suggested by *Roger et al.*, [1994]. According to this study, a "flow channel event" that consists of a rapid plasma jet can cause a plasma depletion in the cusp region. When IMF B_z is consistently negative, a region of enhanced plasma density in the cusp is isolated. This higher-density region then

Paper number 96JA03141.
0148-0227/97/96JA-03141$09.00

drifts more poleward if IMF B_y changes from negative to positive thus forming a patch.

Although it has been more than 2 decades since the first observation of patches, a relatively objective definition has just recently been put forward by *Coley and Heelis* [1995] in order to conduct a statistical study using the DE 2 database. According to this study, a nonlocally produced plasma enhancement drifting antisunward in the polar cap qualifies as a patch if it has two edges in which the plasma density is enhanced above 40% in 140 km, and the overall enhancement must be larger than 100% above the background. The parameters defining a patch can of course be changed, but under these conditions, results indicate that 281 such patches were encountered with an average horizontal scale size of 300-400 km, when structures with scale sizes larger than 1250 km are considered to comprise the background. It is also reported that patches are a winter phenomena, and they are mostly observed between 1200 and 2000 UT.

Smaller-scale structures associated with patches were first reported by *Weber et al.* [1986]. They showed that the patches were almost always accompanied by small-scale (<1 km) ionospheric irregularities which cause scintillation at 250 MHz. Furthermore, their results include a weak indication of stronger scintillation on the trailing edge of the patch. This is found to be consistent with E×B drift instability [*Linson and Workman*, 1970]. However, *Linson and Workman* [1970] conclude that the presence of irregularities on the leading edge and throughout the interior of all of the patches may suggest a generation of irregularities by a dominant electrostatic turbulence process. *Basu et al.* [1990] studied structuring by the gradient drift instability and velocity shear driven processes at high latitudes. The former is driven by a large density gradient in a homogeneous convection field with respect to the neutrals, and the latter is driven by a structured convection field in an ambient ionosphere where density fluctuations exist. It is reported that the magnitude of the electric field perturbation was at least 1 order of magnitude larger in velocity shear driven processes when compared to the ones with gradient drift instability. It is also reported that considering the magnitude of the electric field perturbation as well as spectral shapes is crucial in determining the type of instability that is at work.

The object of this paper is to study the smaller scale kilometer-size structure seated on large gradients associated with polar ionization patches. Unlike previous attempts by *Weber et al.* [1984] and *Basu et al.* [1990], our aim is to make use of a quantitative patch definition that recently became available and to study the structure on patches identified by this criteria. We chose to limit our study to noon-midnight-aligned passes of the spacecraft both to keep the material manageable and also to make use of the fact that the E×B drift of the plasma is in many cases approximately parallel to the spacecraft look direction in this meridian. This makes it possible to associate the horizontal velocity structure with the observed structure in ion density and draw conclusions regarding the well-known instability processes such as the gradient drift instability. We describe some common characteristics in structure seen on patches throughout the polar cap and also point out the presence of some rare cases.

2. Data and Method of Analysis

Patches that are studied in detail here were identified by the algorithm proposed by *Coley and Heelis* [1995] (hereafter referred to as paper 1). The criteria they used to identify these patches were briefly explained in the previous section. According to this algorithm, a nonlocally produced density enhancement qualifies as a patch when it has gradients larger than 40% in 140 km on both edges, and the total enhancement must exceed 100% above the background. Examination of the electron temperature is used to establish the absence of electron precipitation. This study was limited to the northern hemisphere in order to exclude any hemispherical differences. Since local time and season were locked together in DE 2, the spacecraft was in a noon-midnight-aligned orbit twice a year during northern summer (August) and winter (March). Throughout the 20-month lifetime of the spacecraft between August 1981 and February 1983, March 1982 was the only time when the spacecraft was in a noon-midnight aligned orbit in winter. The patches we study in detail are from a 40-day period starting on March 1, 1982.

The data used in this study were provided by the retarding potential analyzer (RPA) and the ion drift meter (IDM) on board the DE 2 spacecraft. The DUCT sensor on the RPA measures the total ion concentration from which the structure in this parameter can be measured with high sensitivity [*Hanson et al.*, 1981]. The ion current to the collector is measured 64 times/s, giving an ion density measurement approximately every 120 m of flight path. This allows us to resolve stationary structures with scale sizes down to 240 m. On the other hand, IDM measures two mutually perpendicular angles of arrival of thermal ions with respect to the sensor look direction [*Heelis et al.*, 1981]. These measurements are then used to derive two components of the ambient thermal ion drift velocity. IDM provides the absolute measure of the ion arrival angle 4 times/s and measurements of the angle relative to an absolute value, established every 8 s, at the rate of 32 samples/s. This corresponds to one measurement approximately every 240 m for each direction allowing a spatial resolution of stationary structures with scale sizes down to 480 m.

The structure in the ion density and velocity is described by the spectral content in the time series of measurements. An example of total ion density measurements made by the RPA in the northern hemisphere polar cap during orbit 3133 of DE 2 is displayed with full resolution (64 Hz) in Figure 1a. The density enhancement observed at 0408 UT when the spacecraft was at a very high latitude in the nightside polar cap qualifies as a patch according to the definition used in paper 1. Throughout this patch, which extends 502 km along

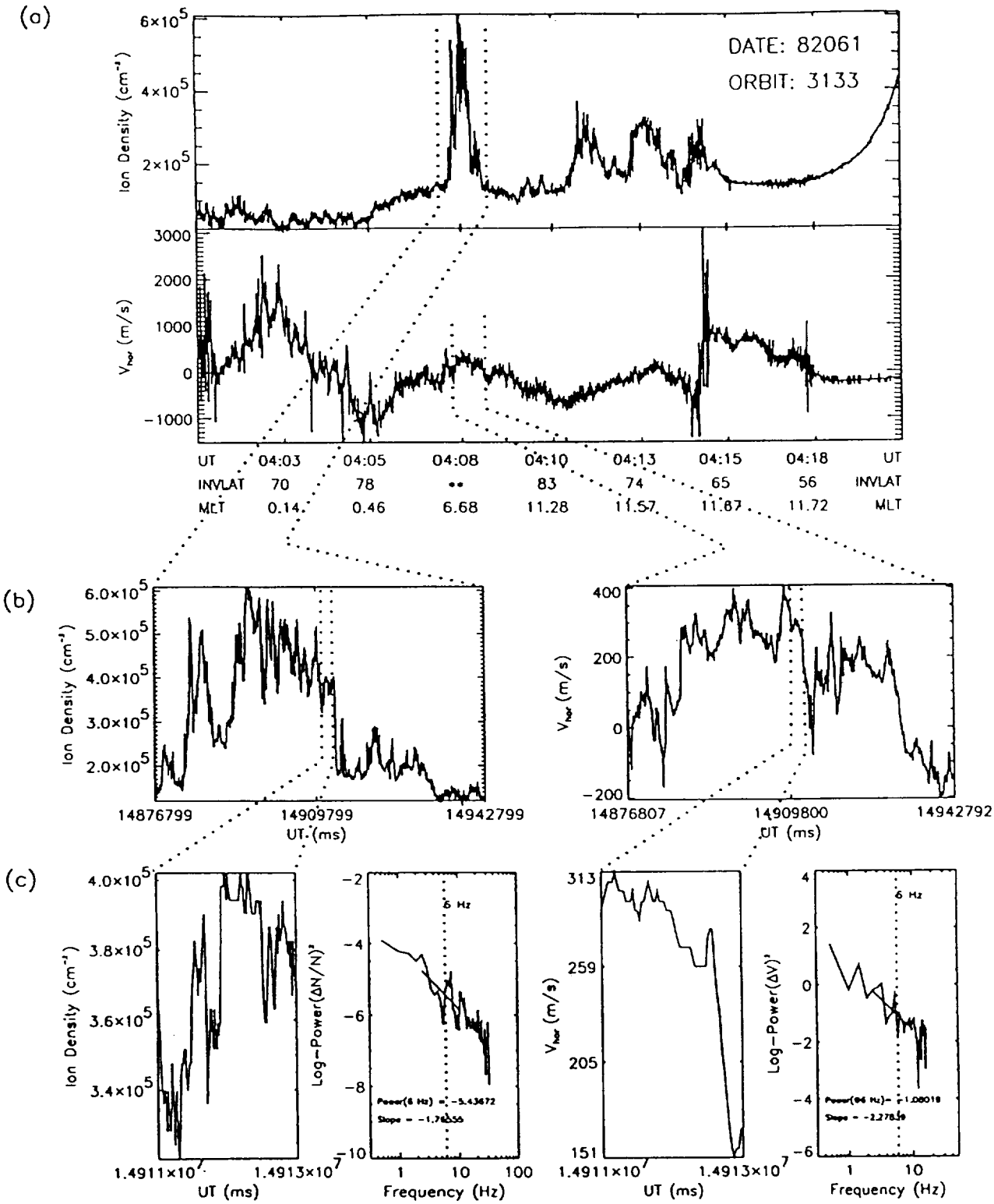

Figure 1. (a) High-resolution (64 Hz) ion density and (32 Hz) horizontal velocity data from orbit 3133 of DE 2. (b) A smaller 500-km segment of the same data associated with the patch at 0408 UT plotted separately. (c) 2-s segments of ion density and velocity data together with their power spectra.

the satellite track, the ion density changes from about 1.3×10^5 to 5.7×10^5 cm^{-3} with a relative factor $\Delta N/N$ of ≈ 4 above background. Two well-defined edges are seen with respect to a fairly constant background. Several other enhancements are observed throughout the pass, but they do not form patches in the working definition either because the gradients on the edges are not steep enough or the overall enhancements above background are not sufficient.

Figure 1a shows the horizontal ion drift velocity mea-

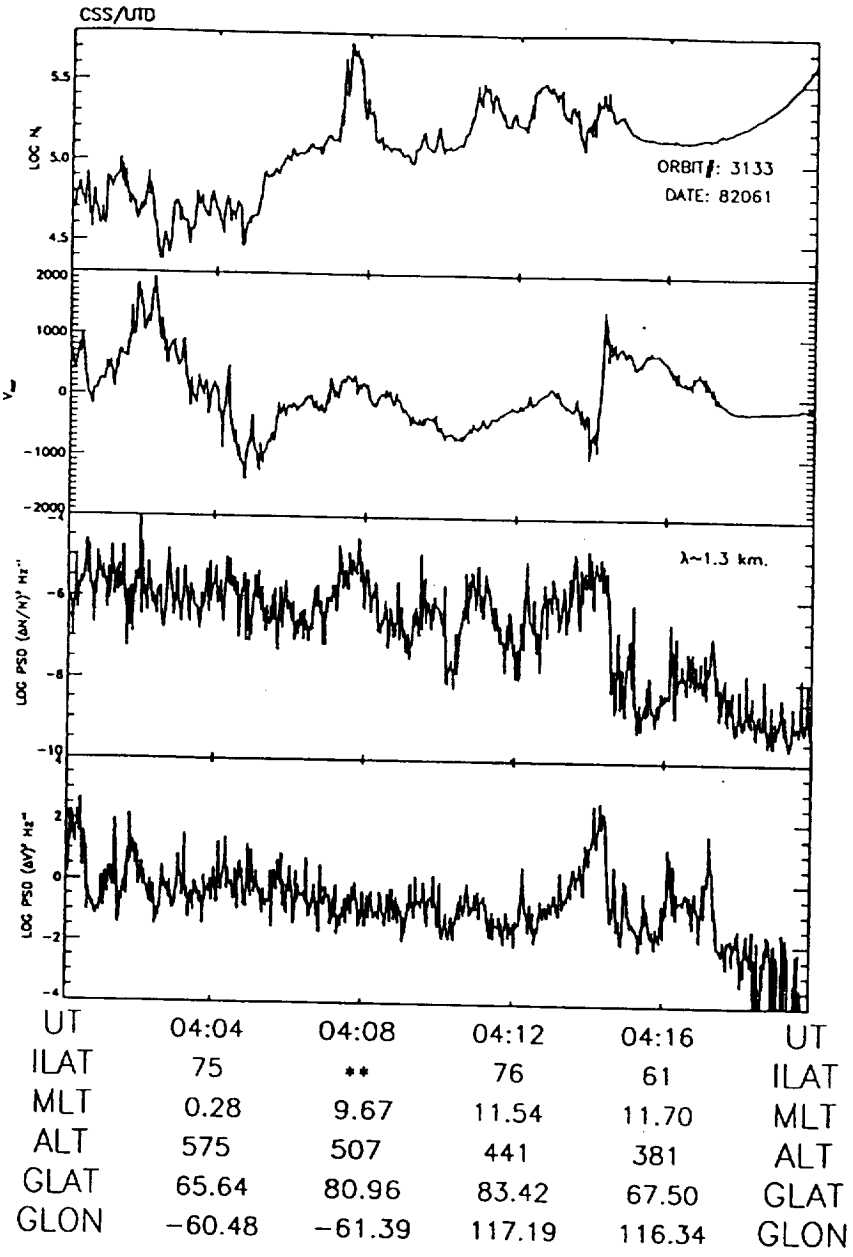

Figure 2. Reduced ion density and horizontal velocity data from orbit 3133. Mean values of the two parameters in each 2-s window are displayed in the upper panels. Lower panels show the power spectral densities at 6 Hz (≈ 1.3 km).

sured by the IDM in 32-Hz resolution. Since the spacecraft is moving approximately parallel to the midnight-noon meridian, this component of the velocity perpendicular to the spacecraft motion is parallel to the dawn-dusk meridian, and the positive values show dawnward motion of plasma in this direction. The patch and the horizontal velocity associated with that segment of the pass are plotted separately in Figure 1b. The presence of smaller-scale structure throughout the patch is observed together with an enhancement of irregularity amplitude on larger gradients. For the analysis of the ion density data, each pass of the high-latitude region is divided into 16 km (2 s) segments and a spectral analysis is performed on each segment.

Examples of such 2-s segments of density and velocity data are displayed in Figure 1c, as are the associated power spectra. A linear detrend is performed on each 2-s segment of ion density data. The slope and the value of the midpoint of the detrend line is recorded respectively as the background slope and the average density for that 2-s segment. The detrend line is also used to calculate the relative change in density ($\Delta N/N$) for each measurement. Power spectral analysis is performed on this quantity from which the power in $\Delta N/N$ at 6 Hz (≈ 1.3 km) scale size and the spectral slope in the 3.1 km to 400 m range is recorded (see Figure 1c).

Velocity data are analyzed in a similar manner, and the power in ΔV at 1.3 km is recorded. As a result of the lower resolution in the velocity data, the spectral slope can be accurately calculated between 3.1 km and 800 m, leaving some margin for high-frequency noise.

Figure 2 shows the derived parameters for ion density and horizontal velocity for the same orbit. The parameters plotted in all four panels are calculated from 2-s data segments using the method explained above. Thus each point in this Figure 2 corresponds to a 2-s segment that consists of 128 (64) measurements of ion density (horizontal velocity). The upper two panels show the mean values of the measured quantities in each 2-s segment. The lower two panels display the power spectral density at 6 Hz ($\approx$ 1.3 km), which corresponds to the value of the fitted line at 6 Hz in the spectra plots of Figure 1c. We use a database of these derived parameters to study the spectral characteristics of polar cap F region irregularities on large gradients associated with polar ionization patches. Although we will primarily use the data associated with segments that comprise a patch in the working definition, it is instructive to first examine a complete high-latitude pass like the one displayed in Figure 2 and to describe the general differences between a patch and its surrounding environment. The study of patches and comparisons among different patches remains our primary concern and will be discussed at length in the following sections of this paper.

From inspection of Figure 2 and almost all other passes throughout the high-latitude ionosphere, it is clear that the intensity in the smaller-scale ($<$ 16 km) structure shows some general characteristics changing with location and solar zenith angle. For the 18 passes in which patches were observed, the intensity of structure showed the following similarities. At 1.3-km scalesize, the high-latitude region above 50° invariant latitude can be divided into three different regions. In decreasing level of structure, these regions are the auroral zone, the polar cap, and the lower latitudes. For a 2-s window and 64 (32) Hz resolution in ion density (velocity), the highest values of power at 6 Hz ($\approx$ 1.3 km) are consistently observed throughout the auroral zone with power spectral densities frequently exceeding -6 in $\Delta N/N$ and $+1$ in ΔV. The values for the polar cap are usually lower with -7 for the ion density and -2 for the velocity. The lowest values that approach the noise floor are found at lower latitudes with spectral densities less than -9 and -2, respectively. Note that the highest power spectral density (PSD) values for velocity at the lower latitudes approach the lowest values seen in the polar cap (about -2), but the PSD values for ion density have 2 orders of magnitude difference for the two regions. Although the highest level of structure is consistently observed at and near the auroral zone for both parameters, occasionally PSDs are seen to reach values up to -4 for the ion density and 3 or 4 for the velocity. One major difference for the two parameters is that these extremely high values of PSD in ion density can be observed everywhere in the polar cap or the auroral zone, whereas they seem to be limited to the auroral zones for the velocity. Note that patches are distinguished by their density enhancement above the background, rather than an enhancement in $\Delta N/N$.

3. Observations

The high-latitude F region of the ionosphere contains structure with scale sizes ranging from thousands of kilometers down to the ion gyroradius. Polar cap ionization patches with scalesizes of a few hundred kilometers are among the largest scale-size structures observed in this region during the nighttime. The object of this paper is to present a detailed study of the smaller kilometer-size structures associated with polar ionization patches identified by the criteria introduced in paper 1.

It is necessary to mention that these patches are not produced locally as a result of energetic particle precipitation. They are usually antisunward convecting, solar-produced density enhancements in the polar cap. The group of patches we are considering is evenly distributed along the noon-midnight meridian with a majority of them residing on the dawnside of this line.

All the patches encountered fall into one of four groups that differ in magnitude and distribution of structure on the patch along the observation direction. In decreasing structure along the patch, these four groups are (1) fully structured patches, (2) patches with structure only on the edges, (3) patches with only one structured edge, and (4) unstructured patches. The majority of the patches we describe belong to one of the first two groups with only single examples in each of the last two groups.

Among the 18 enhancements that qualify as a patch in the working definition, "fully structured patches" are the most common. Figure 3 shows two examples of fully structured patches encountered by DE 2 in the northern winter polar cap. Figure 3a replots the features of the patch described in Figures 1 and 2. Note that the scale on the y axes of the lower two panels are different in Figure 3. We chose to fix the scale in the y axes of these plots in order to make it easier to compare the irregularity amplitudes on different patches. We fix the scale for density irregularities between -4.5, which is approximately the largest observed PSD, and -7.0, which is close to the lowest observed polar cap values above the noise floor. For the ion velocity, the values 0.5 and -2.0 respectively are chosen for the same reasons. The dashed lines at -6.0 and -1.5 in Figure 3 are also plotted to help compare the irregularity amplitudes between different patches. Also indicated in the top panel of Figure 3 are the average convection speeds of the patch feature along the satellite motion (V_{ram}) and perpendicular to the satellite motion (V_{hor}). These parameters are then used to identify leading and trailing edges of patches with respect to their average motion.

The large-scale density features of these patches are reflected in the large-scale velocity features, suggesting that they result from a different convection history

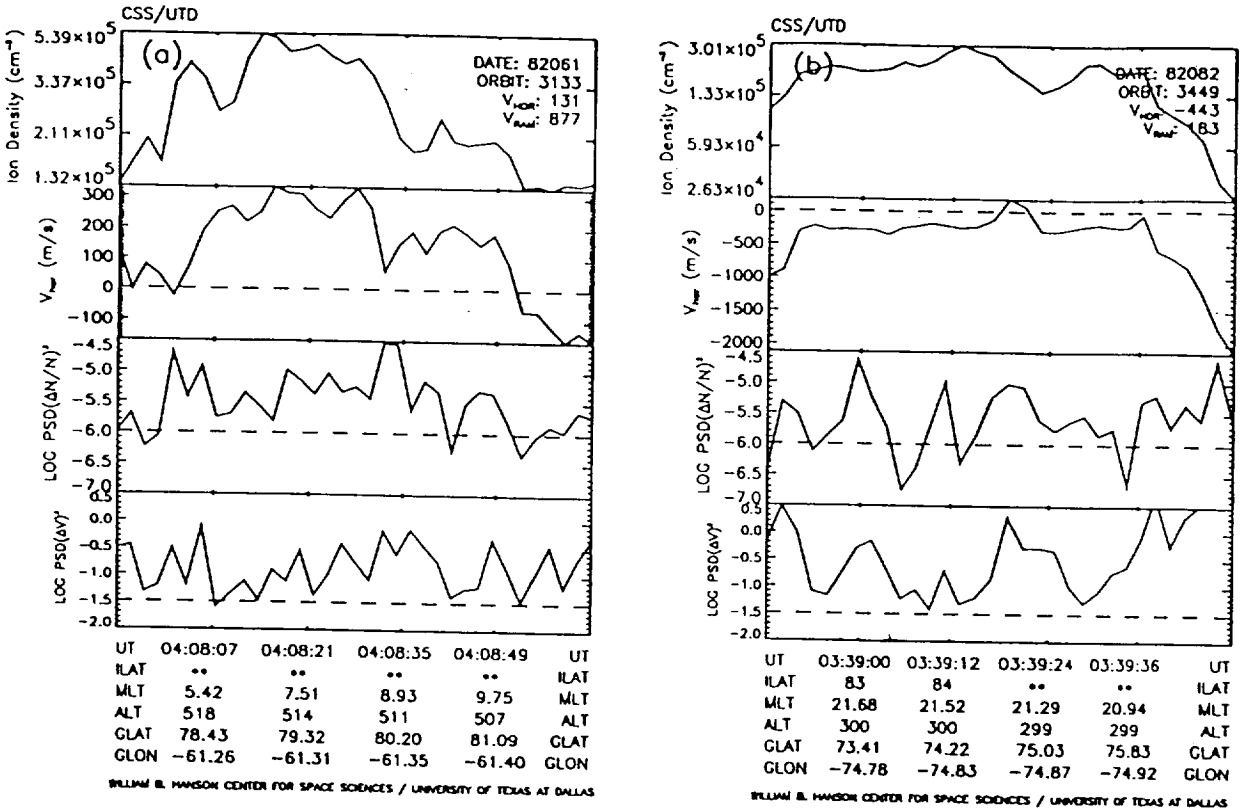

Figure 3. Similar to Figure 2, but only the segment of the data associated with the polar cap ionization patches on orbits (a) 3133 and (b) 3449 are displayed. Fully structured patches.

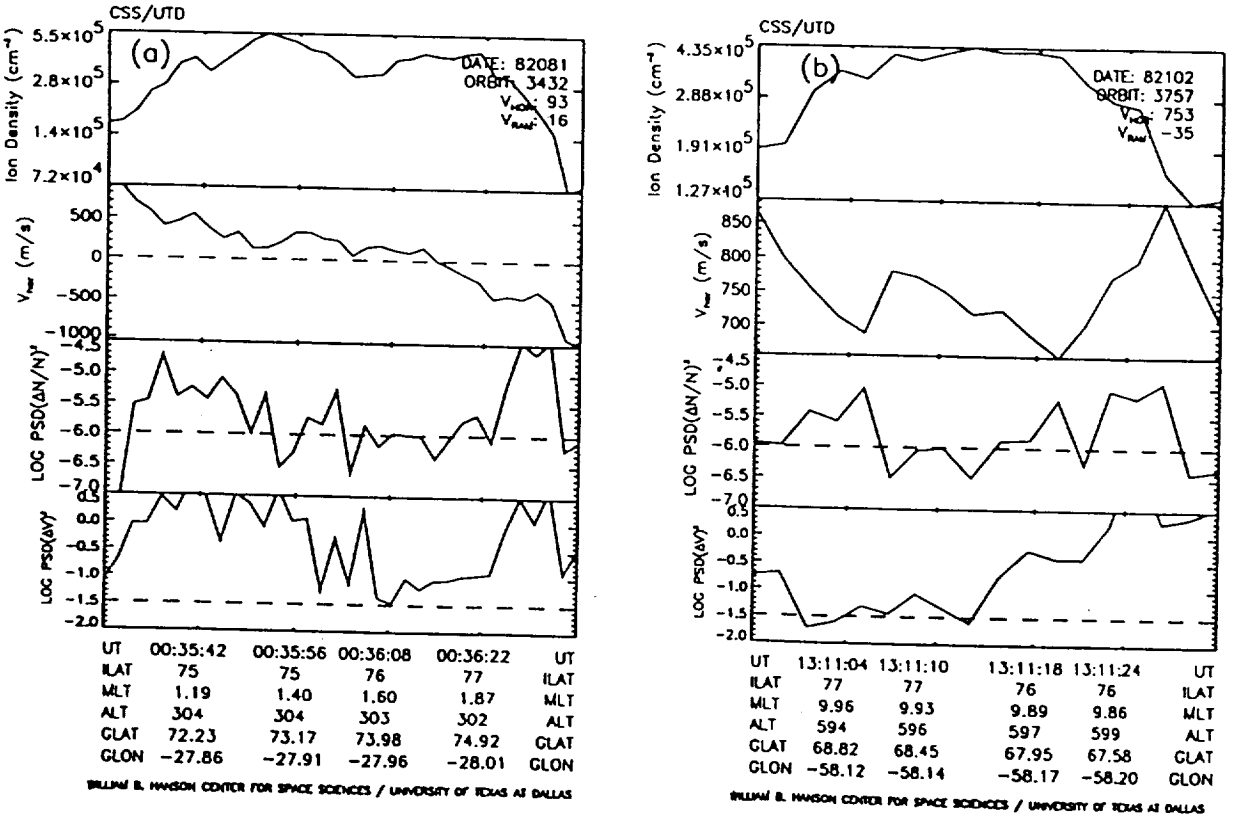

Figure 4. Similar to Figure 3, except for orbits (a) 3432 and (b) 3757. Patches with structure only on the edges.

from the neighboring plasma. As we will see later, this is not a reproducible feature of patches, and thus the patches we observe usually have shapes that are evolving in time. Both patches show the common characteristic of increased level of irregularity amplitude ($\Delta N/N$) throughout the enhancement. This can also be verified by comparing the power in $\Delta N/N$ at 6 Hz ($\approx$ 1.3 km) on the patch and at the vicinity of the patch in Figure 2. There is a considerable amount of structure on both of the edges and also throughout the patch where the background density gradients are smaller than at the edges. It is apparent that the largest values of irregularity amplitude in ion density correspond to the steepest gradients in the ion density, and the values -4.5 to -5.0 are among the highest seen in the patches we studied. The amplitude of structure in the velocity seems to be correlated with that of the density, and powers around -0.5 are seen throughout the patch. For fully structured patches, it is possible to locate the edges of the patch by using the level of structure as an indicator.

Figure 4 shows two examples in the same format as Figure 3 of patches for which the density irregularity intensity is noticeably larger at the edges than in the body of the patch. In Figure 4a, the larger-scale horizontal velocity gradient appears to produce a bifurcation of this patch, and the density irregularity is enhanced at the bifurcation. In Figure 4b, the large-scale horizontal variation is consistent with a differing convection history for the patch. As before, there are regions where the velocity irregularity intensity is loosely correlated with density irregularity intensity, but background density gradients modulate this behavior. It should be noted that the horizontal velocity component perpendicular to the spacecraft track is sometimes comparable to or greater than the along track component. Such is the case in Figure 4b, and in this case, the patch edges cannot be uniquely identified as leading or trailing with respect to the convection direction.

To complete our description of the irregularity features associated with patches, we show in Figure 5, respectively, a patch with enhanced structure on one edge and a benign patch with the lowest level of structure seen in the polar cap. The patch in Figure 5a has a rather small cross track horizontal velocity and is clearly convecting antisunward. The density irregularity power at 6 Hz is consistently under -6 for most of the patch except for two 2-s segments where the power reaches values larger than -4. The high levels of structure appear on the leading edge of the patch and would not therefore support the role of the gradient drift instability. However, knowledge of the neutral wind velocity is required to reach secure conclusions in this regard.

In Figure 5b, the nonstructured patch has two steep gradients defining leading and trailing edges along the satellite track. It resides on the nightside of the dawn-dusk meridian, a significant distance from the dayside cusp where it is assumed to originate. This patch has a cross track horizontal velocity comparable in magnitude

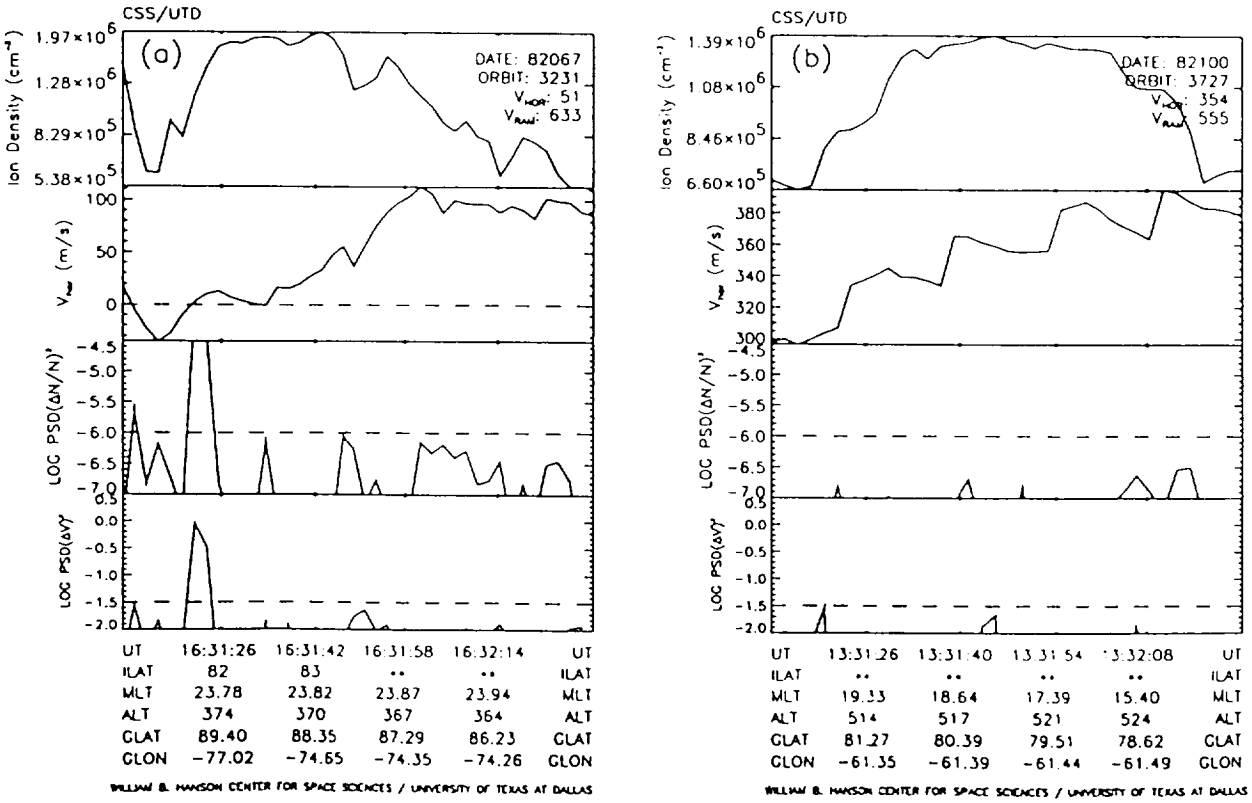

Figure 5. Similar to Figure 3, except for (a) orbit 3231, patch with structure only on one edge and (b) orbit 3727, the benign patch.

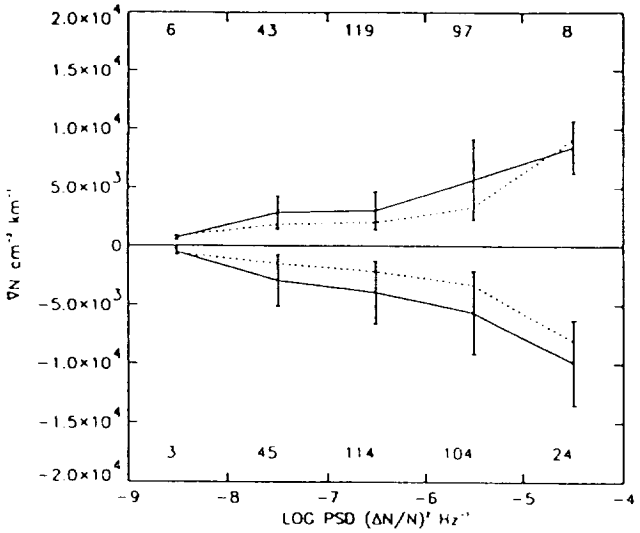

Figure 6. Power spectral densities in $\Delta N/N$ versus ∇N.

to the along track component. Thus, in this case, the patch edges cannot be identified as leading or trailing with respect to the convection direction.

For all structured gradients associated with patches, we have investigated the association between the velocity and density structure in a more quantitative manner. We have noted previously that the relationship between density irregularity intensity and background density gradient is not obviously asymmetric. Figure 6 shows the relationship between these quantities for all patches where the ambient drift measurements allow the identification of leading (positive ∇N) and trailing (negative ∇N) edges with respect to the convection direction. For gradients of each sign, power spectral densities of ion density irregularity at 6 Hz ($\approx$ 1.3 km) are binned and averaged for each decade. The results are plotted with standard deviations and the number of 2-s segments that go into each average. The dashed line connects median values in each bin. As mentioned earlier, knowledge of the neutral wind velocity is required for unequivocal identification, but the behavior shown here and reflected on all observed gradients suggests that the gradient drift instability cannot be readily identified on average although specific cases may be observed.

In the process of describing our observations, we frequently observe a correlation between the irregularity intensity in velocity and density. Further investigation shows that this correlation is modulated by the background gradient in the density. For the purposes of illustration, we have divided all observed density gradients into three groups established by the horizontal gradient-scale length $L = [\nabla N/N]^{-1}$. These three groups with small, medium, and large gradient-scale lengths respectively correspond to less than 83 km, between 83 and 166 km, and greater than 166 km, where according to its definition, the smallest gradient-scale length represents the largest change in density above the background. Figure 7 shows the relationships between irregularity intensities in $\Delta N/N$ and ΔV for each case. The Figure 7a shows the data points and a straight-line fit to these points. For comparison, Figure 7b shows the fitted straight lines. While the linear dependence between these parameters is the same in all cases, we see that for a given velocity irregularity significantly large den-

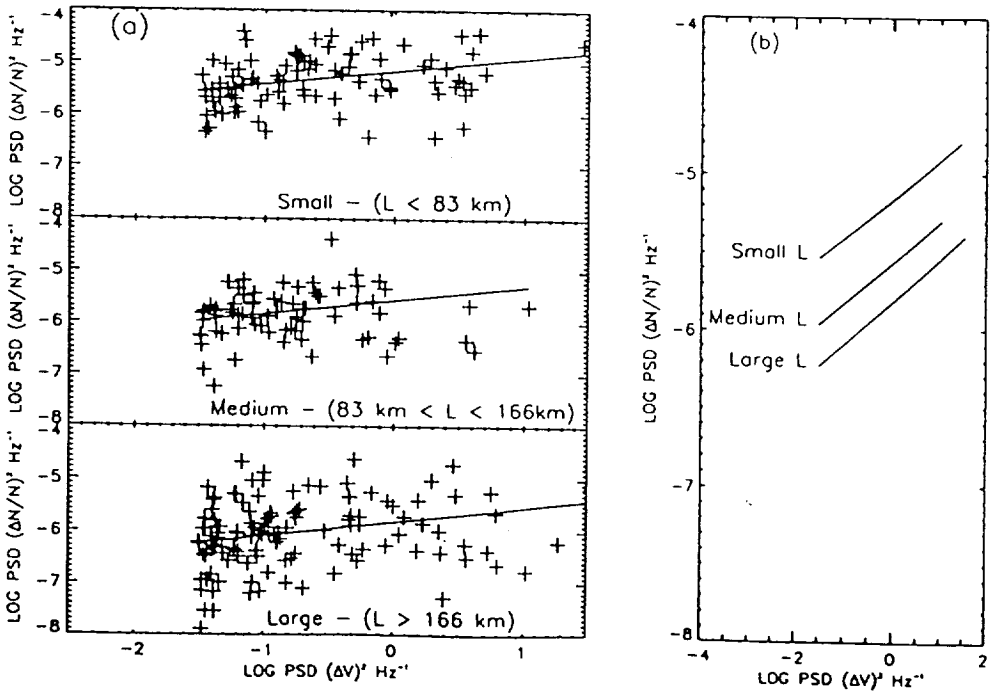

Figure 7. (a) Ratios of powers in $\Delta N/N$ to ΔV for three different L values. (b) Ratios for different L values.

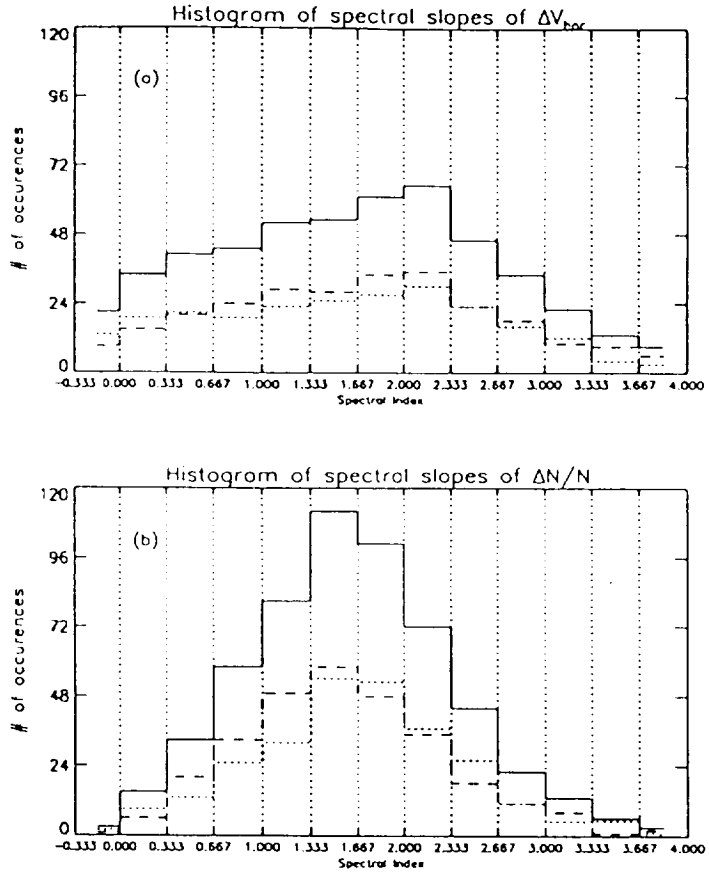

Figure 8. Histogram of spectral slopes for (a) ΔV and (b) $\Delta N/N$. Histograms plotted with dotted lines are for positive gradients and dashed lines are for negative gradients.

sity irregularities are produced in the presence of the largest background density gradients.

Finally, we investigate the spectral index of density and velocity irregularities in polar cap patches. In all there are 563 2-s (16 km) segments comprising all the patches observed. Figure 8 shows the distribution of spectral indices of the density and velocity for all the patches. As we have previously noted, the velocity irregularity intensity is quite small, and fits to a spectral slope may be compromised by the inclusion of points on the noise floor. However, removal of these points confirms that a preponderance for shallow spectral slopes exists even at the highest powers. The distribution of spectral slopes in the velocity structure can be contrasted with a more symmetric and narrow distribution of slopes in the density structure. Furthermore, the spectral indices of the velocity take on larger values than the density. When we take into account the sign of the background gradients, as shown with dotted and broken lines in Figure 8, a slight but clear shift toward larger spectral indices for $\Delta N/N$ occur for positive gradients regardless of which edge they belong to. This may be an indication of the effect of the gradient drift instability superposed on turbulent mixing which may also be effective in producing structure at these scale sizes.

4. Discussion

Patches are generally assumed to be created by temporal variations in the convection patterns of the high-latitude plasma. A region at or near the cusp seems to be the location where such high-density plasma can penetrate into higher latitudes through such a time varying process. Observations show that these patches then drift in the antisunward direction on the nightside. There is some evidence that these patches are later redistributed in the midnight region at auroral zone latitudes in the form of latitudinally confined enhancements that are called the boundary (or subauroral) blobs [*Tsunoda*, 1988].

As these large-scale patches are made and moved around at high latitudes under time varying convection patterns, they carry very large density gradients into the nightside with them. These large gradients that make the edges of the patches are found to be the seat for smaller-scale kilometer-size structures. Flux tube interchange processes such as plasma instabilities or stirring are reported to be among the mechanisms that contribute to the observed structures at these scale sizes. Although there have been some earlier attempts using a few patches [*Basu et al.*, 1990; *Weber et al.*, 1984, 1986] to identify the relative contribution from

these two mechanisms in producing structures at these scale sizes, the dominant one of the two is yet to be determined.

While most qualitative definitions of patches adapted by researchers seem to agree with each other, the lack of a quantitative definition seems to prevent a direct comparison of studies in this field. To overcome the discrepancies, we have used the only relatively objective, quantitative definition to identify the patches that were studied in this paper. Of course, as we mentioned earlier, the presence of a large gradient in density is the primary requirement for small-scale structures to form via an interchange process, but the spatial extent of this enhancement that is vital in the definition of the large-scale patch features is by no means a parameter in the formation of small-scale structures. Ironically, for our study, patches or any other loosely or strictly defined large-scale plasma enhancements are not special in any way for seating small-scale plasma structures. That is, given the same conditions, a 10-km long density gradient is equally capable of producing small-scale structures as a 100-km long patch edge with a similar gradient. The only benefit of concentrating on large-scale patches for our study is to make use of these unusually well-defined edges that give us a very good data set with gradients of various magnitudes under similar background conditions. It should be emphasized that there exists in the polar cap, many equally structured density gradients that do not make up a patch. Significant scintillation associated with patches is a consequence of the dependence of scintillation on ΔN rather than $\Delta N/N$.

Magnetic flux tube interchange processes like stirring or E×B drift instability break large gradients up into smaller-scale structures. In the case of stirring, applied electric fields do not depend on the cusp-patch distance. Furthermore, stirring produces smaller-scale structure on gradients of either sign when structured electric fields are mapped on them. This is different from the behavior expected from a case where the dominant mechanism is an instability process (in the linear regime), where only certain conditions are convenient for the mechanism to become unstable. For example, the E×B drift instability is expected to produce structure on the trailing edge of a patch under B_z negative conditions. Since the patches in the polar cap are usually convecting antisunward during negative B_z, the sunward edges of patches are most likely to be unstable for cases where E×B drift instability is dominant. In fact, if the drift instability is dominant, then we should expect to see patches with larger edge gradients and relatively less structure closer to the cusp. If the conditions are right for perturbations to be unstable, these steep edges should be continuously broken up by the instability mechanism as the level of smaller-scale structure increases toward midnight, resulting in shallower but highly structured trailing edges. Of course, a patch formed in a Chapman F layer will usually have a lifetime of the order of an hour and as is well known, the high-latitude convection patterns can change drastically over this time period. Changes in the patch motion can therefore produce smaller-scale structure on more than one edge given sufficiently large instability growth rates. Thus, in order to identify the working mechanisms that produce structure on an edge, one must consider the convection histories of patches, the size of edge gradients, and relative levels of structure in ion density and horizontal velocity on each edge.

Convection histories are important in order to identify the observed edges as leading or trailing. With one-dimensional measurements made by a spacecraft, the convection velocity of the patch will always have components parallel and perpendicular to the spacecraft path unless the spacecraft is moving exactly in the same direction as the patch. Choice of midnight-noon-oriented passes help in this sense to establish a larger component parallel to the spacecraft path. For slip velocities (V_o) larger than zero, this may give larger V_o/L irregularity growth rates in midnight-noon-oriented gradients (with respect to dawn-dusk-oriented gradients) for similar L values when the sign of the convection velocity is the same as the sign of the gradient. E×B drifting gradients will otherwise be stable. Thus the dominance of this instability mechanism on the edges of patches moving in the noon-midnight direction is more easily studied with passes in the noon-midnight direction when two edges with gradients of opposite sign are encountered over a short distance. A dawn-dusk-oriented component of the convection velocity which may lead to nonzero slip velocities almost always complicates the interpretation of observed characteristics. As this component of the slip velocity becomes comparable to the noon-midnight-aligned component, both leading and trailing edges observed in a noon-midnight-oriented pass will lie on the leading or trailing side of the patch in the dawn-dusk meridian. Thus leading and trailing edges of a patch in the noon-midnight direction may have comparable levels of structure if the spacecraft happens to cross the patch on the trailing edge of the dawn-dusk-oriented motion.

The size of gradients on each edge of a patch and irregularity power at 6 Hz can reveal information on the source of irregularity production. It is quite clear that a patch with large amounts of structure on its edges may not be able to maintain very large edge gradients for a long time. A decrease in the size of edge gradients that is dependent on the sign of the gradient is mostly expected from cases where the drift instability is responsible for the observed structure. One also expects to see an enhancement of small-scale structure on the unstable edge of the patch together with a decrease in the spectral slope. On the other hand, a quantitative comparison of the power in $\Delta N/N$ and ΔV can help identify cases where stirring causes gradients of both signs to become structured.

Observations of polar cap patches with in situ spacecraft measurements show that most patches have an increased level of structure at 1.3-km scale size over the entire enhancement with respect to the background. The power at this scale size peaks at the edges of patches when such edges are clearly defined. Other-

wise, the level of structure on the plateau between the two edges of the patch reaches values approximately equal to those on the edges. On average, there is no significant difference in the level of observed structure on leading and trailing edges. Thus structuring due to an evolving E×B drift instability is not easily observable on the edges of patches. This is either because patches are already created with structure so that the contribution from the drift instability is not as significant as it would be on an unstructured patch, or dominant stirring on both edges of a patch override the present structuring due to the instability, and the resulting level of irregularity is a reflection of the stirring mechanism rather than the instability process. One of the better indications of this is the fact that patches have structure independent of location from the cusp. Although there is a lot of variation in the magnitude of structure from patch to patch, they are found to contain very high levels of structure both very close and also far away from the cusp. There is no general asymmetry in either the density profile or the $\Delta N/N$ power that allows the identification of leading and trailing edges. According to our observations, the irregularity powers seem to favor the larger gradients rather than a specific sign of the gradient. Our results displayed in Figure 6, which are consistent with stirring show that on average the power in $\Delta N/N$ at 6 Hz is an increasing function of the magnitude of the background gradient regardless of its sign.

It is clearly seen from Figure 7 that $\Delta N/N$ is an increasing function of ΔV for a given value of L. The fact that the ratio is larger for larger L values is also consistent with stirring in which a given level of irregularity in ΔV will produce larger $\Delta N/N$ irregularity amplitudes in ion density on gradients with larger L than it will on gradients with small L.

We note that the irregularity intensities in velocity are quite small in patches and comparable to the levels in the surrounding plasma. However, significantly shallower spectral slopes for ΔV within a patch suggest that they are associated with increased velocity structure at the shortest wavelengths (500 m). An increase in density irregularity above the background is the distinguishing feature of a patch. The spectral slopes for the velocity irregularities are generally steeper (-2) than those of the density (-1.7).

Although most of our results support the existence of a stirring mechanism in general, it is clear from some individual cases that an evolving E×B drift instability is active in the polar cap. In fact, the histogram of spectral indices for positive and negative gradients displayed in Figure 8b supports this claim with a slight shift toward higher spectral slopes for positive gradients. This is consistent with increasing powers at smaller scales on negative gradients which generally denote trailing edges of patches that are E×B drift unstable.

Finally, we want to revisit the benign patch in Figure 5b. This is the only patch which was found to contain very low levels of irregularity with two very clearly defined steep edges. An important observation related with this patch was the absence of any large-scale fluctuation in the horizontal velocity. The presence of very clean and steep edges suggests that this patch was not exposed to any kind of structuring earlier in its lifetime. Lack of structure in ΔV, on the other hand, suggests that it was not being stirred at the moment when DE 2 spacecraft went through this patch. The fact that the convection direction of this patch is approximately 45° with respect to the spacecraft may help explain the observations. As we discussed in a previous section, when the spacecraft is not aligned with the convection direction of the patch, it is not safe to assume that the observed edges are leading or trailing. As a matter of fact, both of the observed edges may either be leading or trailing. Since it is clearly seen that stirring is not a factor in this patch, we may conclude that the lack of any structuring may be a result of encountering the patch on the side which is also E×B drift stable.

5. Conclusions

Spectral characteristics associated with polar cap ionization patches show that patches are usually regions of enhanced irregularity at small-($\approx$ 1.3 km) scale size. Observations indicate the presence of structure on almost all patches regardless of the distance between the patch and the cusp where they are believed to develop. Observed characteristics show that the nature of the present irregularities can be more easily explained by a stirring mechanism that results in an enhanced level of structure on both edges of patches. The level of present small-scale structure is an increasing function of the magnitude of the background density gradients regardless of their sign. The nature of the ratios of $\Delta N/N$ and ΔV is also consistent with a stirring mechanism. A slight shift toward larger spectral slopes for positive density gradients suggests that there is a contribution from the E × B drift instability in the resulting structure. While patches provide an easily identifiable source of larger-scale (16 km) density gradients that may be structured, they by no means encompass all structured regions in the polar cap.

Acknowledgments. We thank W. R. Coley for assistance with the identification of ionisation patches used in this work. This work is supported by NASA grants NAGW-4492 and NAGW-4442 at The University of Texas at Dallas.

The Editor thanks J. C. Foster and J. J. Sojka for their assistance in evaluating this paper.

References

Anderson, D. N., J. Buchau, and R. A. Heelis, Origin of density enhancements in the winter polar cap ionosphere, *Radio Sci., 23*, 513, 1988.

Basu, Su., S. Basu, E. MacKenzie, W. R. Coley, J. R. Sharber, and W. R. Hoegy, Plasma structuring by the gradient drift instability at high latitudes and comparison with velocity shear driven processes, *J. Geophys. Res., 95*, 7799, 1990.

Coley, W. R., and R. A. Heelis, Adaptive identification and characterisation of polar ionisation patches, *J. Geophys. Res., 100*, 23819, 1995.

Decker, D. T., C. E. Valladares, R. Sheehan, S. Basu, D. N. Anderson, and R. A. Heelis, Modeling daytime *F* layer patches over Sonderstrom, *Radio Sci., 29,* 249, 1994.

Foster, J. C., and J. R. Doupnik, Plasma convection in the vicinity of the dayside cleft, *J. Geophys. Res., 89,* 9107, 1984.

Hanson, W. B., R. A. Heelis, R. A. Power, C. R. Lippincot, D. R. Zuccaro, B. J. Holt, L. H. Harmon, and S. Sanatani, The retarding potential analyser for Dynamics Explorer - B, *Space Sci. Instrum., 5,* 503, 1981.

Heelis, R. A, W. B. Hanson, C. R. Lippincot, D. R. Zuccaro, L. H. Harmon, B. J. Holt, J. E. Doherty, and R. A. Power, The ion drift meter for Dynamics Explorer - B, *Space Sci. Instrum., 5,* 511, 1981.

Hill, J. R., Sudden enhancements of *F* layer ionisation in polar regions, *J. Atmos. Sci., 20,* 492, 1963.

Kelley, M. C., *The Earth's Ionosphere: Plasma Physics and Electrodynamics*, Academic, San Diego, Calif., 1989.

Keskinen, M. J., and S. L. Ossakow, Theories of high latitude irregularities: A review, *Radio Sci., 18,* 1077, 1983.

Kintner, P. M., and C. E. Seyler, The status of observations and theory of high latitude ionospheric and magnetospheric plasma turbulence, *Space Sci. Rev.,41,* 91, 1985.

Linson, L. M., and J. B. Workman, Formations of striations in ionospheric plasma clouds, *J. Geophys. Res., 75,* 3211, 1970.

Roger, A. S., M. Pinnock, J. R. Dudeney, K. B. Baker, and R. A. Greenwald, A new mechanism for polar patch formation, *J. Geophys. Res., 99,* 6425, 1994.

Sojka, J. J., M. D. Bowline, R. W. Schunk, D. T. Decker, C. E. Valladares, R. Sheehan, D. N. Anderson, and R. A. Heelis, Modeling polar cap F-region patches using time varying convection, *Geophys. Res. Lett., 20,* 1783, 1993.

Tsunoda, R. T., High-latitude *F*-region irregularities: A review and synthesis, *Rev. Geophys., 26,* 719, 1988.

Weber, E. J., J. Buchau, J. G. Moore, J. R. Sharber, R. C. Livingstone, J. D. Winningham, and B. W. Reinisch, *F* layer ionisation patches in the polar cap, *J. Geophys. Res., 89,* 1683, 1984.

Weber, E. J., J. A. Klobucher, J. Buchau, H. C. Carlson Jr., R. C. Livingston, O. de la Beaujardiere, M. Mc Ready, J. G. Moore, and G. J. Bishop, Polar cap *F*-layer patches: Structure and dynamics, *J. Geophys. Res., 91,* 12121, 1986.

Ö. Kivanç and R. A. Heelis, University of Texas at Dallas, William B. Hanson Center for Space Sciences, Box 830688, MS FO23, Richardson, TX 75083-0688. (email: kivanc@utdallas.edu; heelis@utdallas.edu)

(Received August 12, 1996; revised October 7, 1996; accepted October 8, 1996.)